



Sirt6 Deficiency in Microvascular Mural Cells as a Driver of Paracrine Senescence and Impaired Regeneration in Ischemic Limbs (Stage 1 Registered Report)

Hao Yin^{1,*}

Published: April 10, 2026

¹ Western University, 1151 Richmond Street, London, Ontario, Canada, N6A 3K7.

*Corresponding author: hyin9@uwo.ca

ABSTRACT

Peripheral artery disease (PAD) and its severe form, chronic limb-threatening ischemia (CLTI), affect over 200 million people worldwide and represent a major unmet clinical need. Following revascularization, successful limb tissue recovery requires coordinated angiogenesis and myogenesis, yet existing treatments inadequately support these processes. This study investigates the role of Sirtuin 6 (Sirt6) in microvascular mural cells—pericytes and arteriolar smooth muscle cells (SMCs)—in orchestrating ischemic muscle regeneration. We hypothesize that loss of Sirt6 in mural cells triggers an anti-regenerative state by inducing a senescence-associated secretory phenotype (SASP) including extracellular histones, which propagates paracrine senescence, fibrosis, and inflammation in skeletal muscle interstitium. Three aims are proposed: characterizing the senescent phenotype and secretome of Sirt6-deficient mural cells; modeling paracrine effects using a 3D microfluidic co-culture system; and performing bulk RNA-sequencing (RNA-seq) integrated with public single-cell datasets. In combination with hindlimb ischemia data derived from a conditional mural cell-specific Sirt6 knockout mouse model, this work will uncover novel mechanisms of tissue failure in CLTI and identify Sirt6 and extracellular histones as potential therapeutic targets for limb regeneration.

INTRODUCTION

Research Question: Background, Importance, and Relevance

Lower extremity PAD, caused by atherosclerotic narrowing or thromboembolic blockage, affects over 200 million people worldwide.¹ Its severe form, CLTI, leads to impaired muscle function, non-healing ulcers, amputation, and death. Following surgical or endovascular revascularization, successful recovery requires coordinated angiogenesis and myogenesis, which is not adequately supported by current medical management. While many preclinical studies have presented strategies to stimulate angiogenesis, few exhibit translational benefit.³

Microvascular mural cells—arteriolar SMCs and pericytes—stabilize blood vessels, regulate blood flow, and integrate hypoxic, inflammatory, and mechanical inputs, thereby mediating communications with endothelial cells and myogenic progenitors in tissue injury and regeneration.² Recent single-cell/single-nucleus transcriptomics studies provide computational evidence for mural cell communications with myogenic and non-myogenic cells in ischemic



skeletal muscle.^{5,6} Despite this, the specific role of mural cells in limb ischemia regeneration is investigated to a limited extent.⁴

Sirtuin 6 (SIRT6) is a class III NAD⁺-dependent histone deacetylase critical to genomic stability, metabolic homeostasis, and healthy aging.⁷ SIRT6 protects against fibrosis and inflammation across multiple pathogenic contexts, but its specific role in PAD or mouse limb ischemia is unknown. Our pilot data show that adult mice with induced mural cell Sirt6 knockout (KO) exhibit insufficient blood flow recovery, impaired angiogenesis, and enhanced fibrosis in the ischemic hindlimb.

Cellular senescence, characterized by irreversible growth arrest and a pro-inflammatory SASP, is associated with age-related vascular diseases including PAD.^{8,9} In SMCs and mesenchymal lineage cells, Sirt6 is a documented anti-senescent protein and a negative modulator of pro-inflammatory and pro-fibrotic transcriptional programs including NF- κ B and TGF β -SMAD signaling.^{10,11} Our pilot data show that Sirt6-deficient microvascular mural cells are senescent and defective in wrapping regenerating capillaries and arterioles in ischemic hindlimb.

Recently, chromatin components including genomic DNA and histones have been identified as part of the senescence-associated secretome.¹² Cellular uptake of extracellular histones triggers senescence via the cGAS-STING pathway,^{13,14} and extracellular histones act as damage-associated molecular patterns (DAMPs) to evoke sterile inflammation through Toll-like receptors (TLR) 2 and 4.¹⁵ Our pilot data show that Sirt6-null SMCs exhibit increased histone transcripts in culture and elevated cytoplasmic histone content in aortic media in vivo, without exacerbated cell death—suggesting that Sirt6 restricts histone mislocalization or release in mural cells.

The central research question is: Can extracellular histones act as secreted mediators of Sirt6 deficiency-induced paracrine senescence and anti-regenerative signaling in ischemic skeletal muscle?

Hypotheses

H1: Paracrine Senescence

Sirt6 deficiency in microvascular mural cells causes cell-intrinsic senescence and a pro-senescent secretome that induces senescence of neighboring endothelial cells and interstitial fibroblasts.

H2: Extracellular Histones as SASP/DAMP Mediators

Extracellular histones released by Sirt6-null microvascular mural cells function as SASP/DAMP components to amplify senescence, impair angiogenesis, and evoke fibrosis through activation of the cGAS-STING pathway.

Timeline

The project will be completed over 6 months. Months 1–3: Aim 1—senescence and secretome analysis in isolated skeletal muscle microvascular mural cells. Months 4–5: Aim 2—3D microfluidic co-culture of skeletal muscle mural cells with endothelial cells or fibroblasts. Month 6: Aim 3—integrative analysis of bulk transcriptome and secretome data with public single-cell/single-nucleus RNA-seq datasets. This project is part of an ongoing multi-year project in the



Pickering Lab; the proposed work generates proof-of-principle data to be incorporated into the broader program and related manuscript(s).

METHODS

Experimental Design

This study uses primary skeletal muscle endothelial cells, pericytes and fibroblasts isolated from a conditional, inducible, mural cell-specific Sirt6 knockout mouse model (tamoxifen-induced Myh11-CreERT2;Sirt6^{flox/flox}, designated Sirt6-SMKO) and tamoxifen-treated Cre-negative littermate controls. Hindlimb ischemia is induced by femoral artery resection prior to cell isolation. Three aims are organized in parallel: (1) cell-based senescence and secretome characterization; (2) 3D microfluidic co-culture modeling; and (3) bulk RNA-seq with integrative single-cell analysis.

Sample and Statistical Power

Aim 1: N=5 mice per genotype. Based on established protocols, 10–20K PDGFR β + mural cells can be isolated per mouse. Pilot data demonstrate that n=5 independent replicates provide >80% power ($\alpha=0.05$) to detect $\geq 30\%$ difference in SA- β -gal activity.¹⁸

Aim 2: N=6 mice per genotype, yielding 300–600K mural cells for ~30 microfluidic chip channels. Based on published experience with microvessel-on-chip systems,^{19,20} N=5–7 provides >80% power ($\alpha=0.05$) to detect $\geq 30\%$ variation in volume-normalized vessel length.

Aim 3: N=4 mice per genotype for bulk RNA-seq. Public datasets used for integrative analysis: GSE233882 (N=20 PAD, N=12 controls; pooled nuclei) and GSE235143 (N=4 per group; subject-level) from GEO.

Data Collection, Processing, and Planned Analysis

Aim 1: Senescence and Secretome Characterization

Microvascular mural cell isolation: following hindlimb ischemia, PDGFR β + cells are isolated from ischemic hindlimb calf skeletal muscle (gastrocnemius, tibialis anterior, soleus) using an established MACS protocol with enzymatic digestion.¹⁶ Cell identity is validated by immunostaining for PDGFR β , NG2 (positive) and CD31, CD45, PDGFR α (negative).

Senescence characterization: primary cultured mural cells are assessed for SA- β -gal activity, p16Ink4a, p21Cip1, γ H2AX, Lamin B1, and pan-histone by immunofluorescence. Subcellular histone localization (nucleus, cytoplasm, plasma membrane) is quantified by high-resolution confocal microscopy.

Secretome analysis: conditioned media from Sirt6-SMKO versus control cells are analyzed by Luminex multiplex assay (RayBiotech) for canonical SASP factors (IL-1 α , IL-6, CCL2, TNF, MMP3) and by ELISA for secreted histones (H2A, H2B, H3, H4). Cell death is monitored by lactate dehydrogenase assay and annexin IV/propidium iodide staining.



Paracrine senescence assay: conditioned media are transferred to (1) control mural cells, (2) C57BL/6N primary skeletal muscle endothelial cells, or (3) C57BL/6N primary skeletal muscle fibroblasts. Recipient cells are assessed for senescence markers.

Mechanistic experiments: conditioned media are depleted of histones using histone-neutralizing antibodies (H3 + H2A/H4) or defibrotide (an FDA-approved polyanionic oligonucleotide that neutralizes histones¹⁷) prior to transfer; isotype IgG or vehicle serves as control. DNase I treatment tests the contribution of histone-associated chromatin DNA. Recipient cells are also pretreated with cGAS inhibitor (RU.521) or STING inhibitor (C-176) or their siRNAs to interrogate the cGAS-STING axis. Sirt6 dependence is validated by adenoviral Sirt6 overexpression rescue.

Aim 2: 3D Microfluidic Co-Culture

Mouse skeletal muscle endothelial cells are seeded in the central channel of fibrin hydrogel (AIM Biotech idenTx Chip) co-seeded with Sirt6-null or control mural cells at a 5:1 endothelial-to-mural cell ratio, perfused with VEGF-A165-containing media for 7 days. Angiogenesis metrics are quantified by confocal microscopy: volume-normalized vessel length, junction density, lumen size, network connectivity, permeability (40 kDa FITC-dextran leakage), basement membrane deposition, and SM α -actin+ mural cell investment.

In a parallel fibrogenesis setup, CellTracker Deep Red-prelabeled skeletal muscle fibroblasts are incorporated at a 5:1 endothelial-to-fibroblast ratio alongside mural cells. Fibrotic phenotype is assessed by immunofluorescence for collagen I, SM α -actin, and lysyl oxidase (LOX). Collagen organization is analyzed by second harmonic generation imaging under two-photon microscopy.

Paracrine senescence in the 3D niche is detected by p16 and p21 immunofluorescence. The density of senescent cells and the distance between senescent mural cells and nearest senescent versus non-senescent endothelial cells are measured in 3D space. Extracellular histones in the hydrogel are detected by immunofluorescence in fixed chips; chip effluent ELISA is used if immunofluorescent sensitivity is insufficient.

Aim 3: Bulk RNA-Seq and Integrative Analysis

Bulk RNA-seq uses rRNA-depleted total RNA libraries from freshly sorted Sirt6-null and control mural cells (ischemic and contralateral). rRNA depletion retains non-polyadenylated histone mRNAs. Differential gene expression and pathway analyses are performed using standard pipelines; batch effects controlled with the gene-wise linear model batch removal procedure. Primary comparisons: Sirt6 KO versus control. Secondary comparisons: ischemic versus contralateral.

Integrative analysis of public single-cell/single-nucleus datasets (GSE235143 and GSE233882): Three histone gene module scores are computed (canonical histones, H2A variants,²¹ histones plus histone chaperones²²) with cell cycle adjustment. Spearman correlations between Sirt6 counts and histone module scores are computed per cell type and condition. Cell type-specific senescence module scores are computed using SenCID²³ (SID2 for pericytes/SMCs, SID4 for ECs,



SID5 for fibroblasts). cGAS-STING pathway scores are computed using Reactome gene set R-HSA-1834941 and a recently published 9-gene cGAS-STING score.²⁴

Variations from the Intended Sample Size

If mural cell isolation yields are insufficient, additional mice will be added. All sample attrition will be documented with rationale. For the 3D microfluidic system, if endothelial vasculogenesis is suboptimal, co-culture conditions (seeding density, media composition) will be optimized before proceeding to endpoint analysis.

Pilot Data

Strong preliminary data from the Pickering Lab support the central hypothesis. Key findings: (A) More necrotic muscle in Sirt6-SMKO mice (Myh11+ mural cell-specific Sirt6 KO) after hindlimb ischemia. (B) Reduced limb reperfusion in Sirt6 KO mice (laser speckle imaging, 28 days post-ischemia). (C) Defective mural cell investment on small arterioles in day 10 ischemic calf muscle (confocal intravital microscopy; mGFP+ mural cells). (D) Defective pericyte investment on capillaries in day 10 ischemic calf muscle. (E) Enhanced senescence (p16ink4A) of mural cells and neighboring endothelial cells and interstitial fibroblast-like cells in ischemic muscle. (F) Increased extranuclear histone 3 content in thoracic aortas of angiotensin II-infused mice. Quantitative data are published in the theses of Dr. Jason Lee and Ryan Wong (Western University).

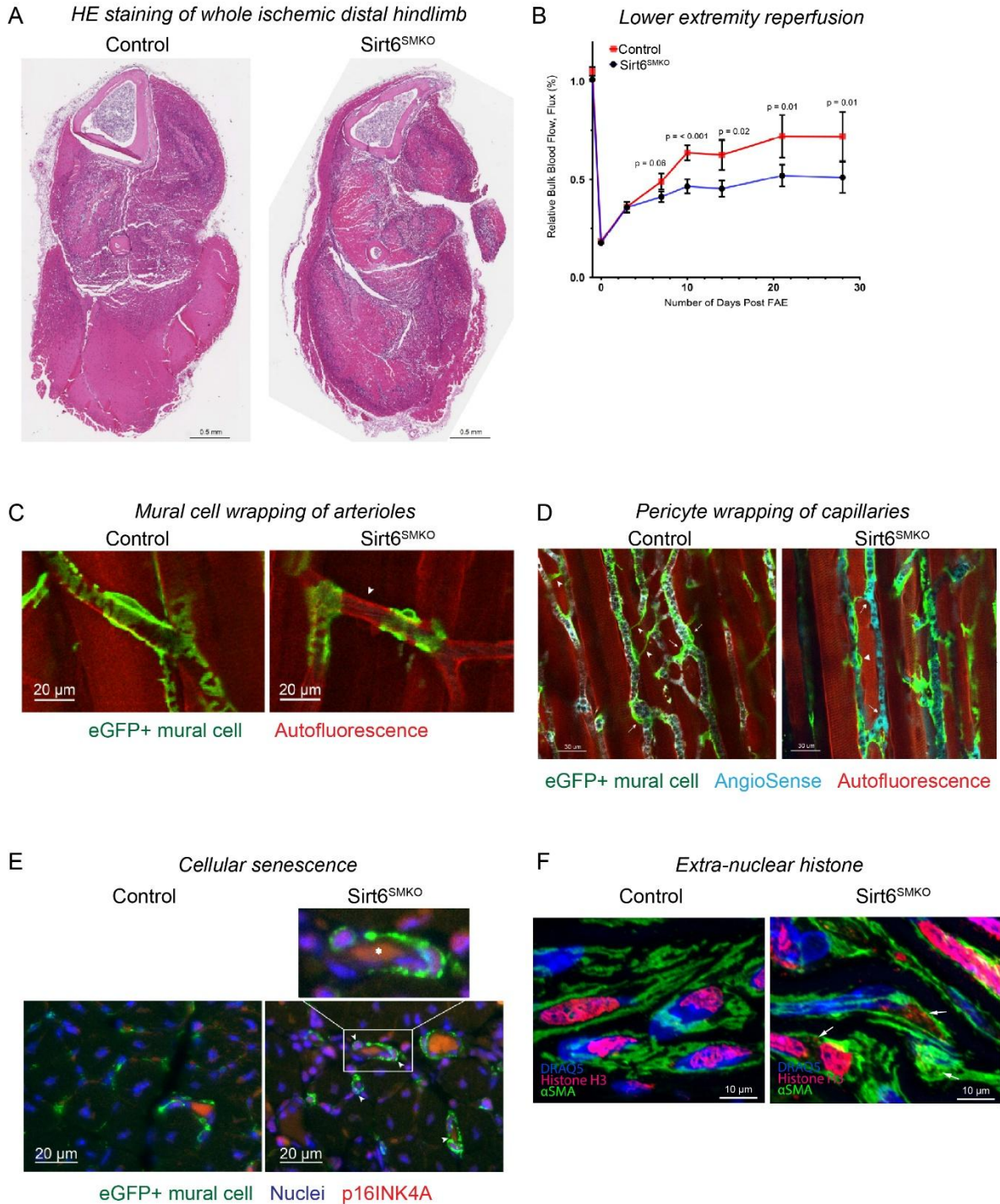


Figure 1. Pilot data demonstrating Sirt6 deficiency-associated phenotypes in ischemic limbs. (A) Hematoxylin and eosin-stained transverse sections showing increased necrotic muscle in Sirt6-SMKO mice 10 days post-ischemia. (B) Laser speckle imaging showing reduced reperfusion in Sirt6 KO mice over 28 days. (C) Confocal intravital microscopy showing defective mural cell wrapping of arterioles (mGFP+, green). (D) Defective pericyte investment on capillaries. (E) Enhanced p16ink4A+ senescence in mural cells and neighboring cells. (F) Increased extranuclear histone 3 in angiotensin II-infused mouse aortas.



Statistical Methods

Aim 1 primary analyses: two-group comparisons (Sirt6-null vs. control; \pm rescue; \pm histone neutralization or cGAS-STING inhibition) by Student's t-test or Mann-Whitney U test depending on data distribution. Secretome multiplexing: Benjamini-Hochberg multiple test correction. Aim 1 secondary analyses: histone subcellular localization across conditions by two-way ANOVA with Sidak's post-hoc correction.

Aim 2 primary analyses: angiogenesis and fibrogenesis metrics by Student's t-test or Mann-Whitney U test. Secondary analyses (paracrine proximity): mixed-effects logistic regression with binary EC senescence as outcome; predictors include distance to nearest senescent mural cell (binned at 10 μ m), Sirt6 mural cell genotype, and genotype \times distance interaction; random effects for experimental replicates; local EC density included as covariate.

Aim 3: differential gene expression by DESeq2 (bulk RNA-seq); Spearman correlation for cell type-specific Sirt6 gene counts and gene set module scores.

Interpreting Results

If H1 is supported (pro-senescent secretome from Sirt6-null mural cells induces paracrine senescence), the findings will define a novel cell-autonomous and paracrine role for SIRT6 in limb ischemia. If H2 is supported (extracellular histones mediate paracrine senescence via cGAS-STING), this will identify histones and cGAS-STING as actionable targets for PAD, and provide rationale for repurposing defibrotide and existing cGAS-STING inhibitors currently in trials for other diseases.

Even if the role of extracellular histones is not confirmed, the secretome, 3D microfluidic, and bulk RNA-seq data will generate new mechanistic hypotheses. Negative results will still substantially advance understanding of mural cell biology in PAD. This proof-of-principle work will be extended by the ongoing multi-year Pickering Lab program, including mouse in vivo validation and human ischemic skeletal muscle tissue analysis.

Dissemination of Information

All analysis R/Python code and raw/processed sequencing datasets will be deposited in public repositories (GitHub, Gene Expression Omnibus [GEO], or Sequence Read Archive [SRA]). Results will be disseminated through peer-reviewed publications and conference presentations.

Study Status

This study has not commenced. At the time of submission, pilot data have been generated and are described above, but the proposed experimental aims have not been initiated. The proposed timeline begins following Stage 1 peer review acceptance.

OTHER REQUIRED INFORMATION

Acknowledgements

The authors thank Dr. Jason Lee and Ryan Wong for contributions to pilot data generation at Western University.



Funding

This work is supported by a ResearchHub grant. This proposal is part of an ongoing multi-year project in the Pickering Lab at Western University; personnel costs are covered by the Pickering Lab.

Author Contributions

H.Y. conceived and designed the proposed study. H.Y., research staff and trainees in Dr. J. Geoffrey Pickering group will perform all proposed experiments and analyses. H.Y. wrote the manuscript. J. Geoffrey Pickering provided scientific supervision, laboratory infrastructure, access to Western University core facilities, and the Myh11-CreERT2;Sirt6^{flox/flox} mouse model. H.Y. read and approved the final manuscript.

Corresponding author: Hao Yin, Western University, 1151 Richmond Street, London, Ontario, Canada, N6A 3K7.

Ethical Approval

Animal Research: Ethics approvals for the use of animal tissue, cells, and adenovirus are in place at Western University Animal Care and Use Committee, in accordance with the Canadian Council on Animal Care (CCAC) guidelines.

Conflicts of Interest

The authors declare no conflicts of interest.

REFERENCES

1. Fowkes, F.G.R. et al. Peripheral artery disease: epidemiology and global perspectives. *Nat. Rev. Cardiol.* 14, 156–170 (2017).
2. Fazio, A. et al. Signaling role of pericytes in vascular health and tissue homeostasis. *Int. J. Mol. Sci.* 25, 6592 (2024).
3. Annex, B.H. & Cooke, J.P. New directions in therapeutic angiogenesis and arteriogenesis in peripheral arterial disease. *Circ. Res.* 128, 1944–1957 (2021).
4. Teng, Y.-C. et al. Analyses of the pericyte transcriptome in ischemic skeletal muscles. *Stem Cell Res. Ther.* 12, 183 (2021).
5. Pass, C.G. et al. Single-nuclei RNA-sequencing of the gastrocnemius muscle in peripheral artery disease. *Circ. Res.* 133, 791–809 (2023).
6. Turiel, G. et al. Single-cell compendium of muscle microenvironment in peripheral artery disease reveals altered endothelial diversity and LYVE1+ macrophage activation. *Nat. Cardiovasc. Res.* 4, 1221–1240 (2025).
7. Korotkov, A., Seluanov, A. & Gorbunova, V. Sirtuin 6: linking longevity with genome and epigenome stability. *Trends Cell Biol.* 31, 994–1006 (2021).



8. Chen, M. et al. Senescent macrophages promote age-related revascularization impairment by increasing antiangiogenic VEGF-A165B expression. *Aging Cell* 24, e70059 (2025).
9. Gremmels, H. et al. Neovascularization capacity of mesenchymal stromal cells from critical limb ischemia patients is equivalent to healthy controls. *Mol. Ther.* 22, 1960–1970 (2014).
10. Kawahara, T.L.A. et al. SIRT6 links histone H3 lysine 9 deacetylation to NF-kappaB-dependent gene expression and organismal life span. *Cell* 136, 62–74 (2009).
11. Maity, S. et al. Sirtuin 6 deficiency transcriptionally up-regulates TGF- β signaling and induces fibrosis in mice. *J. Biol. Chem.* 295, 415–434 (2020).
12. Zaretski, S. et al. Senescent cells secrete chromatin components via senescence-associated extracellular particles. *bioRxiv* 2025.12.12.694055 (2025). doi:10.64898/2025.12.12.694055
13. Dou, Z. et al. Cytoplasmic chromatin triggers inflammation in senescence and cancer. *Nature* 550, 402–406 (2017).
14. Wang, H. et al. Cellular uptake of extracellular nucleosomes induces innate immune responses by binding and activating cGMP-AMP synthase (cGAS). *Sci. Rep.* 10, 15385 (2020).
15. Xu, J. et al. Extracellular histones are mediators of death through TLR2 and TLR4 in mouse fatal liver injury. *J. Immunol.* 187, 2626–2631 (2011).
16. Yin, H. et al. Fibroblast growth factor 9 imparts hierarchy and vasoreactivity to the microcirculation of renal tumors and suppresses metastases. *J. Biol. Chem.* 290, 22127–22142 (2015).
17. Shi, H. et al. Endothelium-protective, histone-neutralizing properties of the polyanionic agent defibrotide. *JCI Insight* 6, e149149 (2021).
18. Vafaie, F. et al. Collagenase-resistant collagen promotes mouse aging and vascular cell senescence. *Aging Cell* 13, 121–130 (2014).
19. González-Gallego, J. et al. A fully iPSC-cell-derived 3D model of the human blood-brain barrier for exploring neurovascular disease mechanisms and therapeutic interventions. *Nat. Neurosci.* 29, 479–492 (2026).
20. Wan, Z. et al. A robust vasculogenic microfluidic model using human immortalized endothelial cells and Thy1 positive fibroblasts. *Biomaterials* 276, 121032 (2021).
21. Yin, X. et al. The function of H2A histone variants and their roles in diseases. *Biomolecules* 14, 993 (2024).
22. Hammond, C.M. et al. Histone chaperone networks shaping chromatin function. *Nat. Rev. Mol. Cell Biol.* 18, 141–158 (2017).



23. Tao, W., Yu, Z. & Han, J.-D.J. Single-cell senescence identification reveals senescence heterogeneity, trajectory, and modulators. *Cell Metab.* 36, 1126–1143.e5 (2024).
24. Chen, Y. et al. Macrophage STING signaling promotes fibrosis in benign airway stenosis via an IL6-STAT3 pathway. *Nat. Commun.* 16, 289 (2025).
25. Chevalier, J. et al. Obstruction of small arterioles in patients with critical limb ischemia due to partial endothelial-to-mesenchymal transition. *iScience* 23, 101251 (2020).